J|A|C|S COMMUNICATIONS

Published on Web 12/06/2010

From Metal−Organic Squares to Porous Zeolite-like Supramolecular Assemblies

Shuang Wang,[†] Tingting Zhao,[†] Guanghua Li,[†] Lukasz Wojtas,[§] Qisheng Huo,[†] Mohamed Eddaoudi,*[,‡] and Yunling Liu*[,†]

State Key Laboratory of Inorganic Synthesis and Preparative Chemistry, College of Chemistry, Jilin University, Changchun 130012, P. R. China, KAUST Advanced Membranes and Porous Materials Center, Chemical and Life Sciences and Engineering Division, 4700 King Abdullah University of Science and Technology, Thuwal 23955-6900, Kingdom of Saudi Arabia, and Department of Chemistry, University of South Florida, 4202 East Fowler Avenue, CHE205, Tampa, Florida 33620-5250, United States

Received November 6, 2010; E-mail: yunling@jlu.edu.cn

Abstract: We report the synthesis, structure, and characterization of two novel porous zeolite-like supramolecular assemblies, **ZSA-1** and **ZSA-2**, having zeolite gis and rho topologies, respectively. The two compounds were assembled from functional metal−organic squares (MOSs) via directional hydrogen-bonding interactions and exhibited permanent microporosity and thermal stability up to 300 °C.

Metal−organic frameworks (MOFs) are an emerging class of solid-state materials that hold promise to solve many key challenging societal needs (e.g., hydrogen storage, carbon dioxide capture, renewable catalysts, controlled drug delivery).[1−3] A subclass of MOFs that are of particular interest are zeolite-like metal−organic frameworks (ZMOFs). These hybrid organic−inorganic porous solids resemble inorganic zeolites in their topologies, a unique feature of which is forbidden self-interpenetration. This advantage offers the potential to construct porous solids with extra-large cavities via decoration and/or expansion of a given zeolite net. Our group, among others, has developed and introduced strategies to form ZMOFs based on the assembly of (i) rigid and directional single-metal-ion tetrahedral building units[4] or (ii) functional metal−organic cubes (MOCs).[5] As expected, these ZMOFs lack interpenetration, possess extra-large cavities and three-dimensional channels, and allow ionic exchange.[6−8]

Our continuous efforts to develop new strategies for the design and construction of functional porous solids such as ZMOFs have led us to explore the utilization of other molecular building blocks. A survey of zeolite topologies revealed that the four-membered ring (4R) is the most abundant secondary building unit (SBU) in conventional zeolites (over 76 zeolite structures are based on the 4R SBU).[9] Thus, functional metal−organic squares (MOSs) would be logical targets as rigid and directional square building units for the synthesis of new zeolite-like supramolecular assemblies (ZSAs) if the MOSs can be designed and programmed to contain complementary peripheral functional groups[10] that can permit and direct their assembly into zeolite-like topologies via supramolecular interactions (e.g., hydrogen bonding).

In order to construct a suitable functional MOS, we opted to use imidazoledicarboxylate-like ligands as bridging linkers because of their unique potential to offer peripheral uncoordinated oxygen centers when chelated to a metal ion in N,O-bis(monodentate) fashion, as previously observed in MOCs.[5] Additionally, bis(monodentate) diamines were employed as capping ligands because they introduce additional hydrogen-bonding sites on the periphery of the molecular squares, which are necessary for the assembly of ZSAs via predictable N−H···O hydrogen bonds.

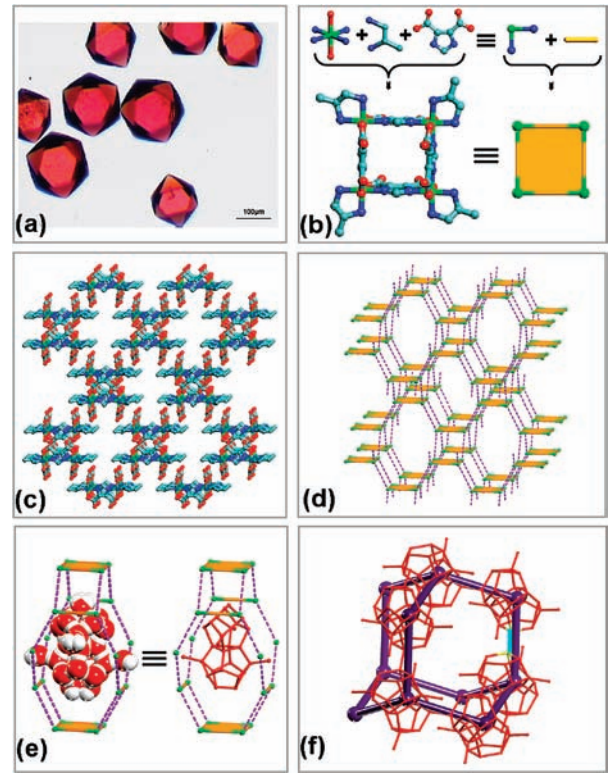

Figure 1. (a) Optical image of **ZSA-1** crystals. (b−f) Crystal structure of **ZSA-1**: (b) ball-and-stick and schematic representations of the MOS SBU; (c) stick model of the 3D framework showing the openings; (d) schematic representation of the gis topology showing the hydrogen bonds and MOS SBUs; (e) CPK (left) and stick (right) models of the $(H_2O)_{28}$ cluster in each gis cage; (f) water cluster network having a diamond topology (the light-blue stick shows the connection, via a hydrogen bond, of two neighboring water clusters). Color code in (b−f): carbon, gray; nitrogen, blue; oxygen, red; cobalt, green; H bonds, purple dots.

Indeed, reactions of 4,5-imidazoledicarboxylic acid (H_3ImDC) and $Co(CH_3COO)_2 \cdot 4H_2O$ under hydrothermal conditions in the presence of 1,2-propanediamine (1,2-PDA) yielded red polyhedral crystals (53% yield based on Co) that were designated as **ZSA-1** (Figure 1a). The as-synthesized compound, which is stable in water and most organic solvents, was characterized by single-crystal X-ray diffraction studies

[†] Jilin University.
[‡] King Abdullah University of Science and Technology.
[§] University of South Florida.

10.1021/ja109980c

and can be formulated as $|(H_2O)_{28}|[Co_4(C_5HN_2O_4)_4(C_3H_{10}N_2)_4]$ (see the Supporting Information).

In the crystal structure of **ZSA-1**, each Co^{3+} ion is octahedrally coordinated in a *trans*-CoN_4O_2 manner with two nitrogen and two oxygen atoms from two individual chelating μ_2-$ImDC^{3-}$ ligands and two N atoms of a single chelating 1,2-PDA molecule. Each $ImDC^{3-}$ ligand connects two Co^{3+} ions in a bis(bidentate) mode. Thus, four 1,2-PDA molecules serving as terminal ligands (i.e., caps) in combination with four Co^{3+} ions and four bridging $ImDC^{3-}$ ligands generate a metal−organic square in the *ab* plane that can be regarded as a 4R building unit (Figure 1b). The orientation of the $ImDC^{3-}$ ligands alternates to form a calixarene-like 1,3-alternating atropisomer molecular square, where the vertices of the square are occupied by four Co^{3+} ions. The regularity of the square is indicated by the fact that the vertex angles are 90° and the Co−Co distances along the edge are 6.003 Å, showing no deviations from the ideal square geometry (Figure 1b).

The two oxygen atoms of each $ImDC^{3-}$ ligand and the two nitrogen atoms of each 1,2-PDA ligand pointing outward from each vertex of each square form four intermolecular hydrogen bonds with the corresponding nitrogen/oxygen atoms of the neighboring square (see Figure S6 in the Supporting Information). Each MOS is connected via 16 hydrogen bonds to four neighboring squares in a tetrahedral geometry (two up and two down with respect to the central square). The molecular squares are positioned parallel to each other and form ladderlike chains via edge-to-edge intermolecular N−H···O hydrogen bonds [2.945(3) Å], generating a 3D network with the zeolite gis topology (Figure 1c,d). The **ZSA-1** framework contains one type of cage (a 4^68^4 gis cage enclosed by 20 Co centers) that generates two intersecting orthogonal channels with approximate dimensions of 12.987 Å × 8.708 Å along the *a* and *b* axes (see Figure S7). A very interesting structural feature of **ZSA-1** is its accessible voids: connection of the cavity centers generates a diamond net (i.e., the dual net of gis is diamond if the 4R windows are not inaccessible), which promotes a diamondlike hydrogen-bonded arrangement of water clusters, each formed in a gis cage and further interconnected through each of the four eight-membered windows.

Each gis cavity encapsulates a water cluster, $(H_2O)_{28}$, formed by cooperative hydrogen-bonding interactions with an average O···O distance of 2.781(3) Å. This value is very close to the corresponding value of 2.759 Å found in I_h ice at −90 °C (see the Supporting Information).[11] Each $(H_2O)_{28}$ cluster can be viewed as two fused cages built from five tetrameric water rings and 12 pentameric water rings, with four additional water molecules on its periphery (Figure 1e and Figure S8). To the best of our knowledge, the observed water arrangement in the gis cage of **ZSA-1** is unprecedented.[12]

Furthermore, each water cluster is interconnected with four neighboring clusters through O4−H···O4 hydrogen bonds [2.807(8) Å] to generate a 3D water network having a diamond topology (Figure 1f and Figure S8).

Reaction of 1,2,3-triazole-4,5-dicarboxylic acid (H_3TzDC), $In(NO_3)_3 \cdot 4H_2O$, and KNO_3 in an *N*,*N*-dimethylacetamide (DMA)/acetonitrile (CH_3CN) solution in the presence of 1,2-diaminocyclohexane (1,2-DACH) afforded yellow rhombododecahedral crystals (64% yield based on In) that were designated as **ZSA-2** (Figure 2a). The as-synthesized compound, which is insoluble in water and common organic solvents, was characterized by single-crystal X-ray diffraction studies and can be formulated as $|K_3(NO_3)_3(H_2O)_{2.5}(CH_3CN)_3|[In_4(C_4N_3O_4)_4(C_6H_{14}N_2)_4]$ (see the SI).

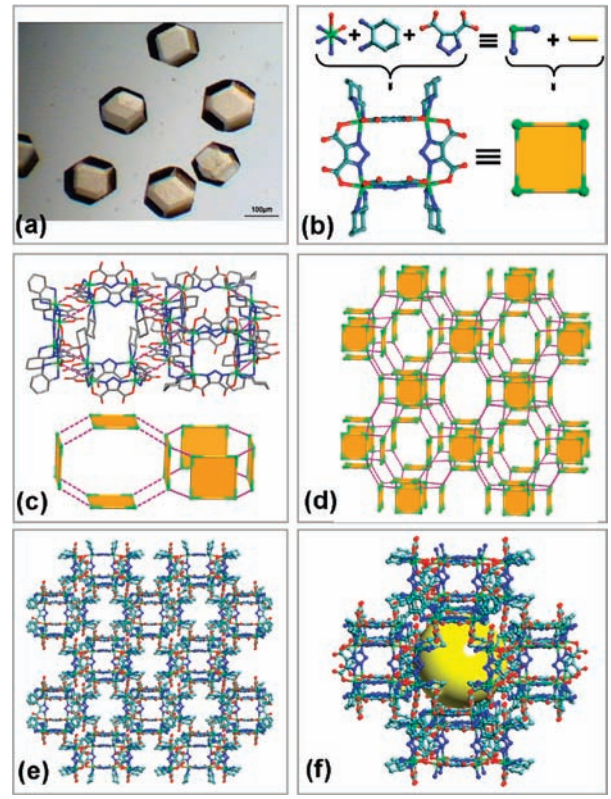

Figure 2. (a) Optical image of **ZSA-2** crystals. (b−f) Crystal structure of **ZSA-2**: (b) ball-and-stick and schematic representations of the MOS SBU; (c) stick and schematic representations of the fused double-eight-membered rings; (d) schematic representation of the rho topology showing the hydrogen bonds and MOS SBUs; (e) stick model of the 3D framework showing the openings; (f) a rho cage formed by 16 MOSs, wherein the yellow sphere represents the largest sphere that can fit inside the cage on the basis of van der Waals radii. K atoms, nitrate anions, and guest molecules have been omitted for clarity.

In the crystal structure of **ZSA-2**, each In^{3+} ion is octahedrally coordinated in a *cis*-InN_4O_2 manner with two nitrogen and two oxygen atoms from two individual chelating μ_2-$TzDC^{3-}$ ligands and two N atoms of a single chelating 1,2-DACH molecule (Figure 2b). Each $TzDC^{3-}$ ligand connects two In^{3+} ions in a bis(bidentate) fashion. Thus, four 1,2-DACH molecules serving as terminal ligands in combination with four In^{3+} ions and four $TzDC^{3-}$ ligands generate a metal−organic square that can be regarded as a 4R building unit (Figure 2b) having In−In distances along the edges of 6.618 and 6.681 Å and vertex angles of 90°. Two opposite $TzDC^{3-}$ ligands (at the 1 and 3 positions) are positioned in the plane of the square and perpendicular to the two other ligands (at the 2 and 4 positions and both on the same side of the MOS, i.e., cis). Each MOS is connected via 16 hydrogen bonds to four neighboring squares in a tetrahedral geometry (two up and two down with respect to the central square). The molecular squares are oriented orthogonal to each other and form double-eight-membered rings via edge-to-edge intermolecular N−H···O hydrogen bonds [2.893(3) and 2.962(4) Å], generating a 3D network with the zeolite rho topology (Figure 2c−e and Figure S9). Each rho cage has an accessible cavity void that can accommodate a sphere with a maximum diameter of 13.73 Å on the basis of the van der Waals radii of the surrounding atoms (Figure 2f).

It should be mentioned that the orientation and configuration of the ligands composing the molecular squares (including the peripheral moieties) in **ZSA-1** and **ZSA-2** are distinct from previously reported metal−organic squares (see Figure S10).[13]

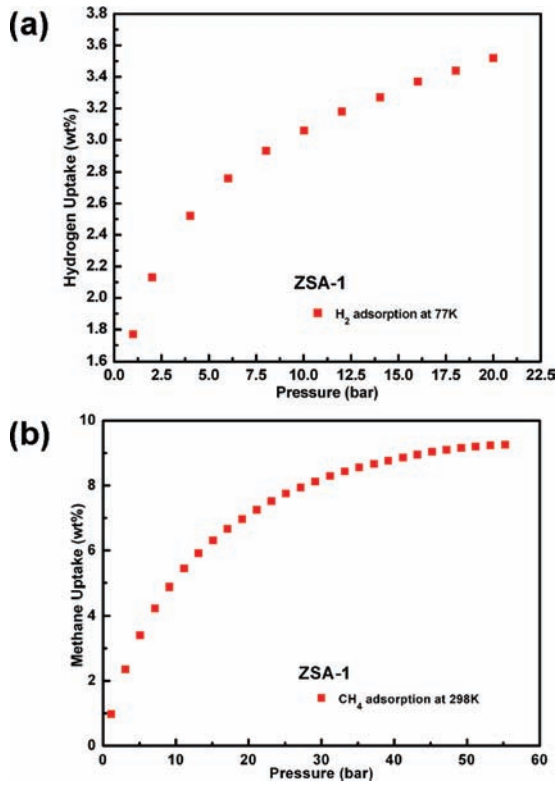

Figure 3. (a) Hydrogen sorption isotherm for **ZSA-1** at 77 K and (b) methane sorption isotherm for **ZSA-1** at 298 K.

The total solvent-accessible volumes for **ZSA-1** and **ZSA-2** were estimated to be 50 and 34.2%, respectively, using PLATON.[14]

The framework thermal stability and structural integrity upon removal of guest molecules were evaluated using powder X-ray diffraction (PXRD) studies. Both **ZSA-1** and **ZSA-2** maintained their crystallinity upon heating to temperatures up to 300 °C and full removal of solvent guest molecules (Figure S4). It should be noted that the cell volume of **ZSA-1** decreased from 7518 to 6505 $Å^3$ upon removal of the guest water molecules (a 13.5% volume reduction). The simulated structure of the activated **ZSA-1** suggests stronger intermolecular N−H···O hydrogen-bonding interactions between neighboring MOSs, as the bond length is reduced from 2.95 to 2.78 Å (Figure S6). The fully evacuated **ZSA-1** regains its original expanded structure upon immersion in water for several minutes or exposure to water vapor for several hours (Figure S11). The maximum water sorption uptake for **ZSA-1** was estimated from the water sorption isotherm to be 380 mg/g (Figure S12).

Nitrogen sorption studies on both **ZSA-1** and **ZSA-2** at 77 K revealed reversible type-I isotherms characteristic of microporous materials (Figure S13). The estimated Brunauer−Emmett−Teller (BET) surface areas for **ZSA-1** and **ZSA-2** were found to be 1382 and 395 m^2/g, respectively, and the corresponding pore volumes were 0.67 and 0.19 cm^3/g.

High-pressure gas sorption measurements were carried out to explore the potential of **ZSA-1** and **ZSA-2** as gas storage materials for H_2 and methane. At 298 K and 80 bar, the total H_2 sorption capacities were 0.50 and 0.35 wt %, respectively, for **ZSA-1** and **ZSA-2** (Figure S14). At 77 K and 20 bar, the total H_2 sorption capacities were 3.5 and 0.95 wt % for **ZSA-1** and **ZSA-2**, respectively (Figure S15). The methane sorption capacity for **ZSA-1** at room temperature and 35 bar was estimated to be 140 v/v(STP) (Figure 3). The observed high methane capacity for **ZSA-1** can be attributed to its narrow pores [average pore size = 5.3 Å as calculated using the Horvath−Kawazoe equation (see Figure S13)], cavity geometry, and relatively higher surface area.

The successful synthesis of the two porous solids **ZSA-1** and **ZSA-2** confirms the potential of our proposed approach for the construction of porous zeolite-like supramolecular assemblies from MOS (4R) building units. Careful choice of the bridging ligands and the chelating agents is critical for the assembly of molecular squares into supramolecular structures with zeolite topologies via directional hydrogen-bonding interactions. Research to extend this approach based on the assembly of molecular squares into supramolecular structures with zeolite topologies to include other functional diamine chelating agents as well as other bifunctional bridging ligands is in progress.

Acknowledgment. We gratefully acknowledge the financial support of the Natural Science Foundation of China (Grants 20701015, 20788101, and 21071059).

Supporting Information Available: Experimental details, PXRD and IR data, TGA curves, structure figures, and X-ray crystallographic data (CIF). This material is available free of charge via the Internet at http://pubs.acs.org.

References

(1) (a) Moulton, B.; Zaworotko, M. J. *Chem. Rev.* **2001**, *101*, 1629–1658. (b) Kitagawa, S.; Kitaura, R.; Noro, S. I. *Angew. Chem., Int. Ed.* **2004**, *43*, 2334–2375. (c) Phan, A.; Doonan, C. J.; Uribe-romo, F. J.; Knobler, C. B.; O'Keeffe, M.; Yaghi, O. M. *Acc. Chem. Res.* **2010**, *43*, 58–67. (d) Férey, G. *Chem. Soc. Rev.* **2008**, *37*, 191–214. (e) Li, J. R.; Kuppler, R. J.; Zhou, H. C. *Chem. Soc. Rev.* **2009**, *38*, 1477–1504. (f) Murray, L. J.; Dincă, M.; Long, J. R. *Chem. Soc. Rev.* **2009**, *38*, 1294–1314.

(2) Lee, J. Y.; Farha, O. K.; Roberts, J.; Scheidt, K. A.; Nguyen, S. T.; Hupp, J. T. *Chem. Soc. Rev.* **2009**, *38*, 1450–1459.

(3) (a) Horcajada, P.; Serre, C.; Vallet-Regi, M.; Sebban, M.; Taulelle, F.; Férey, G. *Angew. Chem., Int. Ed.* **2006**, *45*, 5974–5978. (b) Huxford, R. C.; Rocca, J. D.; Lin, W. *Curr. Opin. Chem. Biol.* **2010**, *14*, 262–268.

(4) (a) Liu, Y. L.; Kravtsov, V. Ch.; Eddaoudi, M. *Angew. Chem., Int. Ed.* **2008**, *47*, 8446–8449. (b) Sava, D. F.; Kravtsov, V. Ch.; Nouar, F.; Wojtas, L.; Eubank, J. F.; Eddaoudi, M. *J. Am. Chem. Soc.* **2008**, *130*, 3768–3770. (c) Liu, Y. L.; Kravtsov, V. Ch.; Larsen, R.; Eddaoudi, M. *Chem. Commun.* **2006**, 1488. (d) Nouar, F.; Eckert, J.; Eubank, J. F.; Forster, P.; Eddaoudi, M. *J. Am. Chem. Soc.* **2009**, *131*, 2864–2870.

(5) (a) Alkordi, M. H.; Brant, J. A.; Wojtas, L.; Kravtsov, V. Ch.; Cairns, A. J.; Eddaoudi, M. *J. Am. Chem. Soc.* **2009**, *131*, 17753–17755. (b) Sava, D. F.; Kravtsov, V. Ch.; Eckert, J.; Eubank, J. F.; Nouar, F.; Eddaoudi, M. *J. Am. Chem. Soc.* **2009**, *131*, 10394–10396.

(6) (a) Tian, Y. Q.; Cai, C. X.; Ji, Y.; You, X. Z.; Peng, S. M.; Lee, G. H. *Angew. Chem., Int. Ed.* **2002**, *41*, 1384–1386. (b) Tian, Y. Q.; Zhao, Y. M.; Chen, Z. X.; Zhang, G. N.; Weng, L. H.; Zhao, D. Y. *Chem.—Eur. J.* **2007**, *13*, 4146–4154. (c) Huang, X. C.; Lin, Y. Y.; Zhang, J. P.; Chen, X. M. *Angew. Chem., Int. Ed.* **2006**, *45*, 1557–1559. (d) Férey, G.; Mellot-Draznieks, C.; Serre, C.; Millange, F.; Dutour, J.; Surblé, S.; Margiolaki, I. *Science* **2005**, *309*, 2040–2042. (e) Fang, Q. R.; Zhu, G. S.; Xue, M.; Sun, J. Y.; Wei, Y.; Qiu, S. L.; Xu, R. R. *Angew. Chem., Int. Ed.* **2005**, *44*, 3845–3848.

(7) (a) Hayashi, H.; Côté, A. P.; Furukawa, H.; O'Keeffe, M.; Yaghi, O. M. *Nat. Mater.* **2007**, *6*, 501–506. (b) Wang, B.; Côté, A. P.; Furukawa, H.; O'Keeffe, M.; Yaghi, O. M. *Nature* **2008**, *453*, 207–211. (c) Banerjee, R.; Phan, A.; Wang, B.; Knobler, C.; Furukawa, H.; O'Keeffe, M.; Yaghi, O. M. *Science* **2008**, *319*, 939–943. (d) Banerjee, R.; Furukawa, H.; Britt, D.; Knobler, C.; O'Keeffe, M.; Yaghi, O. M. *J. Am. Chem. Soc.* **2009**, *131*, 3875–3877. (e) Park, K. S.; Ni, Z.; Côté, A. P.; Choi, J. Y.; Huang, R.; Uribe-Romo, F. J.; Chae, H. K.; O'Keeffe, M.; Yaghi, O. M. *Proc. Natl. Acad. Sci. U.S.A.* **2006**, *103*, 10186–10191.

(8) (a) Wu, T.; Zhang, J.; Zhou, C.; Wang, L.; Bu, X.; Feng, P. *J. Am. Chem. Soc.* **2009**, *131*, 6111–6113. (b) Zhang, J.; Wu, T.; Zhou, C.; Chen, S.; Feng, P.; Bu, X. *Angew. Chem., Int. Ed.* **2009**, *48*, 2542–2545. (c) Wu, T.; Bu, X.; Zhang, J.; Feng, P. *Chem. Mater.* **2008**, *20*, 7377–7382.

(9) Baerlocher, C.; McCusker, L. B. Database of Zeolite Structures. http://www.iza-structure.org/databases/ (accessed Nov 3, 2010).

(10) For studies of molecular squares, see: (a) Stang, P. J.; Olenyuk, B. *Acc. Chem. Res.* **1997**, *30*, 502–518. (b) Fujita, M. *Chem. Soc. Rev.* **1998**, *27*, 417–425. (c) Slone, R. V.; Benkstein, K. D.; Bélanger, S.; Hupp, J. T.; Guzei, I. A.; Rheingold, A. L. *Coord. Chem. Rev.* **1998**, *171*, 221–243. (d) Leininger, S.; Olenyuk, B.; Stang, P. J. *Chem. Rev.* **2000**, *100*, 853–908. (e) Northrop, B. H.; Zheng, Y. R.; Chi, K. W.; Stang, P. J. *Acc. Chem. Res.* **2009**, *42*, 1554–1563. (f) Fujita, M.; Tominaga, M.; Hori, A.; Therrien, B. *Acc. Chem. Res.* **2005**, *38*, 371–380. (g) Ruben, M.; Rojo, J.; Romero-Salguero, F. J.; Uppadine, L. H.; Lehn, J.-M. *Angew. Chem., Int. Ed.* **2004**, *43*, 3644–3662.

(11) Eisenberg, D.; Kauzmann, W. *The Structure and Properties of Water*; Oxford University Press: Oxford, U.K., 1969.

(12) Discrete water clusters, including $(H_2O)_n$ (n = 2−8, 10−12, 14−18, 20, 22, 27, 28, 32, and 45), and 1D chain, 1D tape, 1D pipe, 2D layer, and 3D water structures have been observed in various crystalline materials. See: (a) Cheng, L.; Lin, J.-B.; Gong, J.-Z.; Sun, A.-P.; Ye, B.-H.; Chen, X.-M. *Cryst. Growth Des.* **2006**, *6*, 2739–2746, and references therein. (b) Duan, C. Y.; Wei, M. L.; Guo, D.; He, C.; Meng, Q. J. *J. Am. Chem. Soc.* **2010**, *132*, 3321–3330.

(13) In **ZSA-1**, the two pairs of opposite $ImDC^{3-}$ linkers are all vertical with respect to the square plane in an up−up and down−down fashion. In **ZSA-2**, two opposite $TzDC^{3-}$ linkers (at the 1 and 3 positions) are nearly in the plane of the square, while the other two opposite linkers (at the 2 and 4 positions) are perpendicular to the plane of the square (both on same side, i.e., cis). For ligand orientations and configurations in other reported MOSs, see: (a) Zhang, F. W.; Li, Z. F.; Ge, T. Z.; Yao, H. C.; Li, G.; Lu, H. J.; Zhu, Y. Y. *Inorg. Chem.* **2010**, *49*, 3776–3788. (b) Wang, C. F.; Gao, E. Q.; He, Z.; Yan, C. H. *Chem. Commun.* **2004**, 720–721. (c) Yue, Y. F.; Wang, B. W.; Gao, E. Q.; Fang, C. J.; He, C.; Yan, C. H. *Chem. Commun.* **2007**, 2034–2036.

(14) Spec, A. L. *J. Appl. Crystallogr.* **2003**, *36*, 7–13.

JA109980C